

The Radiation Environment and Damage in the CDF Tracking Volume

Richard J. Tesarek, Yuek Chun Chow, Saverio D'Auria, Andrew Hocker, Kostas Kordas, Susan McGimpsey, Ludovic Nicolas, Rainer Wallny, Steven Worm

(CDF Radiation Monitoring Group)

/CDF/DOC/SECVTX/PUBLIC/6761

Abstract—We present direct measurements of the spatial distribution of ionizing radiation and low energy neutrons ($E_n < 200$ keV) inside the tracking volume of the collider detector at Fermilab (CDF). Using data from multiple exposures, the radiation field can be separated into components from beam losses and collisions and can be checked for consistency between the measurements. We compare the radiation measurements with an increase in the leakage currents of the CDF silicon detectors and find reasonable agreement.

Index Terms—Radiation measurement, radiation fields, ionizing radiations, non-ionizing radiations, radiation effects on instruments

I. INTRODUCTION

PRECISION vertex detectors have become a powerful tool in high energy physics for tagging and reconstructing the decays of short lived particles such as beauty and charmed mesons and baryons. The power of these devices arise from their ability to give precise position information at distances of a few centimeters from the interaction region. Unfortunately, these detectors are susceptible to radiation damage which decreases the signal size and increases the overall noise from the detector [1]. With sufficient damage, these devices become essentially non-functional. Because of the high cost of in capital, manpower and time for the construction of such detectors it is necessary to estimate the lifetime of the detector so that a replacement can be prepared. A key ingredient in an estimate of the detector lifetime is the type, amount and distribution of the radiation seen by the detector.

Modern studies of the radiation environment use Monte Carlo techniques with extensive computer modeling of the processes producing radiation. All of these studies use as input previous measurements of the radiation damage profiles in a single

Manuscript received November 7, 2003. This work is supported by the US Department of Energy and the National Science Foundation, the UK Particle Physics and Astronomy Research Council and the Natural Sciences and Engineering Research Council of Canada.

R. J. Tesarek, S. McGimpsey, L. Nicolas are with Fermilab, Batavia, IL 60563, USA

Y.C. Chow and R. Wallny is with the University of California, Los Angeles, CA, 90095, USA

S. D'Auria, L. Nicolas are with the University of Glasgow, Glasgow G12 800, UK

A. Hocker is with University of Rochester, Rochester, NY 14627, USA

K. Kordas is with the University of Toronto, Toronto, Ontario M5S 1A7, CANADA

S. Worm is with Rutgers University, Piscataway, NJ 05549, USA

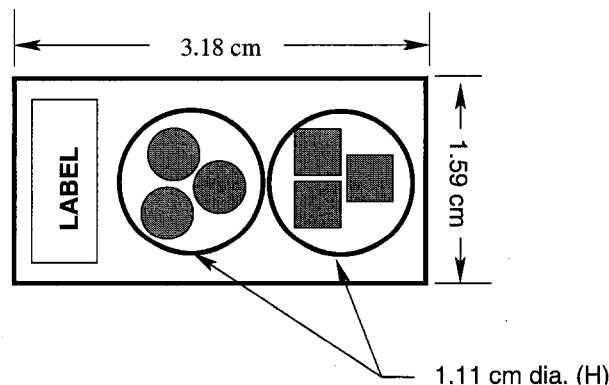


Fig. 1. TLD package made from 0.79 mm thick FR-4 showing TLD-700 (round) and TLD-600 (square) dosimeters. The holes are covered with 76 μm thick kapton tape.

detector published some time ago [2]. In this paper, we present a detailed measurement of the radiation environment seen inside the collider detector at Fermilab (CDF) using thermal luminescent dosimeters (TLDs).

The measurements presented here use Harshaw TLD-700 and TLD-600 [3] types of dosimeters. The TLD-700 dosimeters are made of isotopically pure ${}^7\text{LiF}$ with trace amounts of Mg and Ti and are sensitive to photons and ionizing radiation. TLD-600 dosimeters are made of isotopically pure ${}^6\text{LiF}$ with the same trace elements. Sensitivity to neutrons occurs through the reaction ${}^6\text{Li}(n, \alpha){}^3\text{H}$.

II. MEASUREMENT TECHNIQUE

The radiation field is measured by placing packages of TLD chips at numerous locations in the CDF tracking volume. Each labeled package is made up of a 0.79 mm thick FR-4 holder containing three TLD chips of each type. These chips are held in place with 0.076 mm thick kapton tape. The three chips provide measurement redundancy. To avoid confusing TLDs of different types, each TLD chip type is a different shape. The round TLD-700 chips measured 4.2 mm in diameter by 0.9 mm thick. The square TLD-600 chips measured $3.4 \times 3.4 \times 0.9$ mm³. Figure 1 shows the physical layout of a TLD package.

TLD packages are installed in three regions in the tracking volume. For the first region, packages are placed on the inner faces of the CDF end plug calorimeters, ± 175 cm from the interaction point, at 8 locations in azimuth (ϕ) and 5 locations

in radius (r) from the detector axis (80 locations). For the second region, packages are installed on the outside of the carbon fiber support structure for the inner silicon (SVX, $r = 17.7$ cm) at 5 locations along the detector axis (z) and at 5 locations in azimuth (25 locations). The third region has packages installed on the carbon fiber support structure for the intermediate silicon (ISL, $r = 37.7$ cm) at 5 locations along the detector axis and 8 azimuthal locations (40 locations). The z and ϕ locations for the ISL packages are the same as those for the SVX packages. Additional packages were made and set aside to provide a control dose. A total of 916 dosimeters are used in these measurements.

Installing and harvesting the packages in regions 2 and 3 is accomplished using kapton tape to affix each package to a Mylar leader approximately 6 m long. The ends of the kapton tape are then glued to help keep the tape attached to the leader and smooth the transition between bare leader and leader + tape. This leader is then pulled through eyelets at fixed locations on the carbon fiber support structures. By taping a new leader to the end of an old leader, we install unexposed packages of dosimeters at the same time we harvest exposed packages.

III. CALIBRATION AND DOSIMETRY

The TLD response to photons is measured by exposing each TLD chip to a known dose from a well calibrated source and measuring the light yield as the chip is heated. These calibrations are performed at Fermilab's Radiation Physics Calibration Facility using a 0.010 Gy exposure to a ^{137}Cs source [4]. The neutron response for the TLD-600s is calibrated with a 0.01 Gy exposure to ^{252}Cf at the Oak Ridge National Laboratory Calibration Facility [5]. Approximately 20 neutrons are liberated in the spontaneous fission decay of ^{252}Cf with the neutron energy peaking near 2 MeV [6]. The light yield measurement from each chip is made by the Fermilab radiation safety group using a Harshaw model 2000 TLD reader [7]. The TLD reader records the total charge in nC integrated from a PMT viewing the TLD chip during heating. We find the chip-to-chip variation in photon response to be 2.7% and 3.2% for the TLD-700 and TLD-600 dosimeters, respectively. The photon response of individual TLD chips was found to be reproducible to less than 1%. The chip-to-chip variation in neutron response was measured to be 15% .

The TLDs used for these measurements are known to exhibit superlinearity for doses above 1 Gy; ie, more light is emitted than predicted by a linear model. In order to characterize this non-linearity, we measure the response of a sample of 10 TLD-700 and 10 TLD-600 chips to known photon doses in the range 0.01–100 Gy. The ionizing radiation dose is calculated using the TLD response to a 0.01 Gy exposure and correcting for the non-linearity in TLD response and subtracting the control dose. The neutron dose is calculated by first calculating the normalized response, correcting for non-linearity and subtracting the photon dose from the TLD-700 data. Typical control doses are 0.01–0.1 mGy.

TABLE I
SUMMARY OF BEAM CONDITIONS AT CDF FOR THE THREE TLD EXPOSURE PERIODS.

Period	Beam ($\times 10^{19}$)		Losses ($\times 10^9$)		$\int \mathcal{L} dt$ (pbarn $^{-1}$)
	P	\bar{P}	P	\bar{P}	
Feb. 2001 – May 2001	0.0703	0.0082	15.3	2.02	0.058
May 2001 – Oct. 2001	1.56	0.137	40.9	10.2	12.3
Oct. 2001 – Jan. 2003	96.2	4.89	277.	35.1	167.

IV. MEASUREMENTS

Dosimeters are installed and replaced only during significant periods of accelerator down time. For the data reported here, we include three exposures; February 23 – May 1 of 2001, May 1 – October 8 of 2001 and October 8, 2001 – January 30, 2003. Beam conditions during these exposures are recorded using multiple devices. The number of collisions (accelerator luminosity) is measured at CDF using a device which detects the Cherenkov radiation from charged particles originating from the interaction region [8]. Losses from the proton and antiproton beam are measured using two sets of scintillation counters surrounding the beam pipe and located on either side of the CDF detector. Proton losses are calculated as the coincidence of the counter signals with the timing of protons as they pass the plane of the counters on their way into the CDF interaction region. Similar measurements are made for antiproton losses. Table I summarizes the exposure statistics for the three periods above. From the table, we see that proton losses dominate the first period while proton-antiproton collisions dominate the second and third periods.

Figure 2 shows the ionizing radiation doses for the three exposure periods as a function of the coordinate along the beam line (z). The curves on each plot are to connect the data from measurements taken at different radii from the detector axis. The proton beam travels in the $+z$ direction. Each point on the plot is the average over the ϕ measurements at that z position with uncertainties calculated as the RMS spread of the measurements. Note the different pattern in the z direction in the ionizing radiation for the three periods. The pattern for the collision dominated periods is roughly symmetric about the $z = 0$ while the pattern for the loss dominated period is asymmetric in z . The later pattern is consistent with lost protons and secondaries from beam-gas events being restricted by a small aperture on the $-z$ side of the detector. Antiprotons are expected to produce a similar pattern, but the effect is reduced because the antiproton beam current is an order of magnitude less.

Figure 3 shows the radiation dose for low energy neutrons for the first two periods. Note that the neutron dose in the central part of the detector is independent of position in both periods.

One may assume that the overall radiation environment is a linear super-position of two contributions, one from collisions and the other from losses. For the first two periods listed above, this gives two equations and two unknown distributions. Solving for the two patterns yields the result indicated by

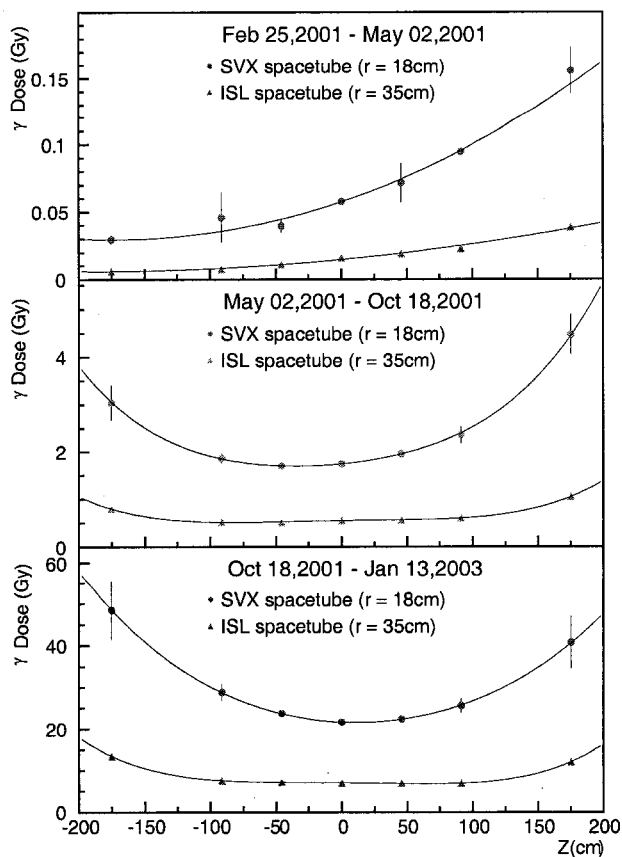


Fig. 2. Ionizing radiation dose as a function of z ; protons travel in the $+z$ direction. The top, middle and bottom plots correspond to the three exposure periods (see Table I). Curves on the plots serve only to guide the eye between measurements at the same radius from the beam.

the closed points in Figure 4. The shaded band in the figure represents the systematic uncertainty on the loss measurement. Good agreement is seen between the collision dose rate separated from the first two periods and the dose rate (raw dose normalized by the luminosity) in the third period as indicated by the open points. One may estimate the fraction of the ionizing radiation from collisions by dividing the raw dose observed in a given period by the product of the collision dose rate and the luminosity. Using this prescription, we find collisions account for 20%, 82% and 91% of the ionizing radiation for the first, second and third exposure periods, respectively. Qualitatively, the increase in the fraction of radiation from collisions improves with the beam conditions. We note here that a substantial period of accelerator studies and beam tuning occurred before the installation of the silicon detectors and radiation monitors.

V. MODELING

In order to predict the radiation seen by various detector components, one needs a model to extrapolate the above measurements to device locations. We use a model based on previous experience from silicon damage profiles measured in the CDF detector [2]. This model assumes that the radiation field surrounding the interaction region is cylindrically sym-

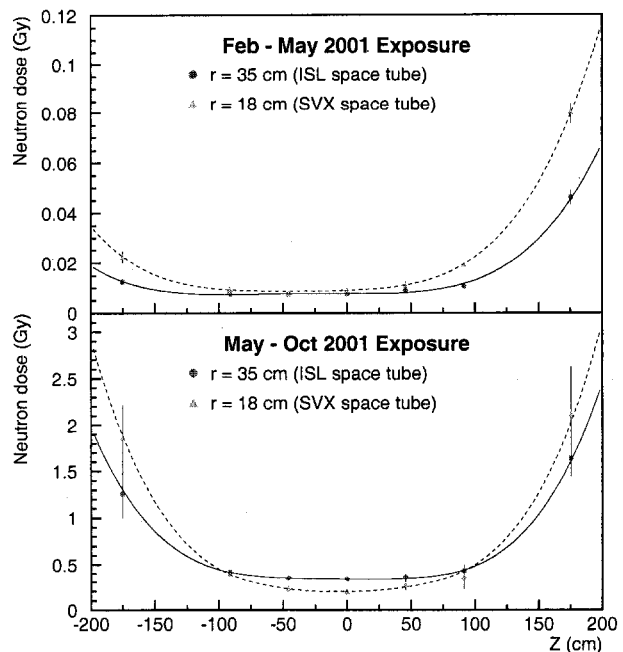


Fig. 3. Neutron radiation dose as a function of z ; protons travel in the $+z$ direction. The top and bottom plots correspond to the first two exposure periods (see Table I). Curves on the plots serve only to guide the eye between measurements at the same radius from the beam.

metric and follows a power law in $1/r$, where r is the distance from the beam axis. We fit the data at each z location to the functional form:

$$D = \frac{A}{\left\{ (x - x_0)^2 + (y - y_0)^2 \right\}^{\frac{\alpha}{2}}}, \quad (1)$$

where A is an absolute normalization, α is the power law and (x_0, y_0) is the beam-detector relative offset. The normalization and power law results are summarized as a function of z in Figures 5 and 6 for the collision and proton loss components of the ionizing radiation field, respectively. We see good agreement between the collision component separated from the first two periods and the data of the third period for the region of the tracking volume occupied by the silicon detectors ($|z| < 100$ cm). We find the value of α for the collision component ranges 1.5 – 1.6 in this region while the loss component in the same region ranges 1.7 – 2.0.

Ultimately, one wishes to compare the radiation field measurements with the damage observed in the detectors. The radiation field predicted by the TLD measurements can be tested by comparing particle fluxes calculated from leakage current measurements in the low radius silicon detectors. The particle flux is calculated by measuring the slope in the silicon leakage current as a function of accelerator delivered luminosity. The rate of increase in the current is corrected from 8° C to 20° C and a damage factor of 3.0×10^{-17} A/cm. The dose rate in the TLDs is converted to a particle flux using the conversion factor of 3.87×10^7 minimum ionizing particles (MIP)/rad and dividing the result by the luminosity for the

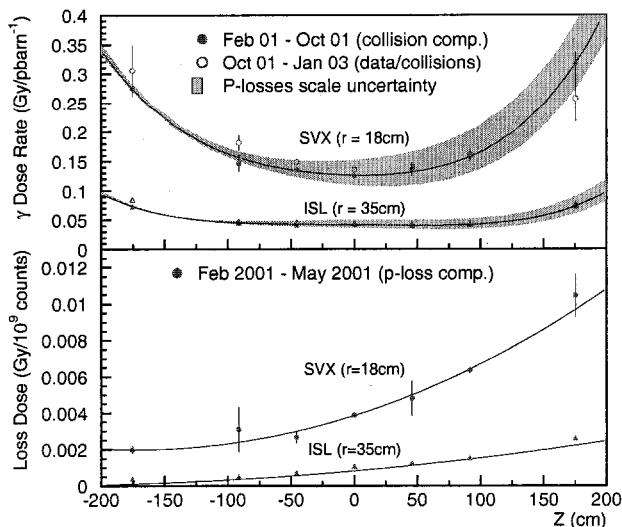


Fig. 4. Ionizing radiation separated into components due to collisions (top) and proton beam losses (bottom). The open points are the raw dose rates from the third period (see Table I).

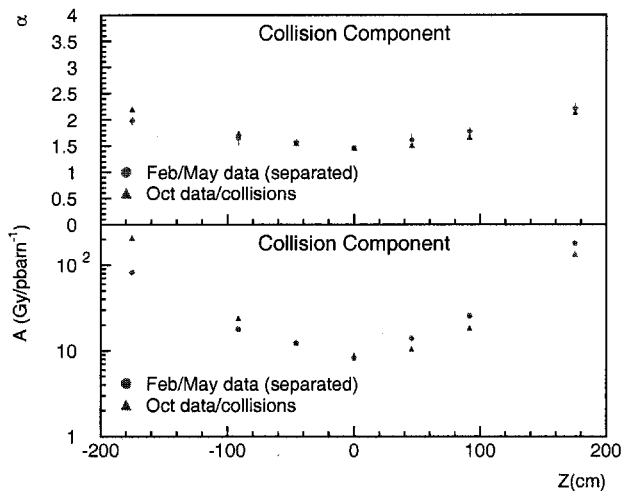


Fig. 5. Fit results for the collision component of the radiation field as a function of z for the last two exposure periods. The top figure shows the power law exponent, α ; the bottom figure shows the normalization, A .

second period (12.3 pbarn^{-1}). Figure 7 compares the particle flux from leakage current data for the innermost layer of silicon ($r = 1.7 \text{ cm}$) with the prediction from the TLD data. The fractional deviation between the two is approximately 10%.

VI. SUMMARY

We use thermal luminescent dosimeters to measure the spatial distribution of the radiation field inside the CDF tracking volume. These measurements include components due to both ionizing radiation and low energy neutrons ($E_n < 200 \text{ keV}$). We find the spatial distribution of ionizing radiation is different for periods dominated by proton beam losses and periods dominated by proton-antiproton collisions. Low energy neutrons

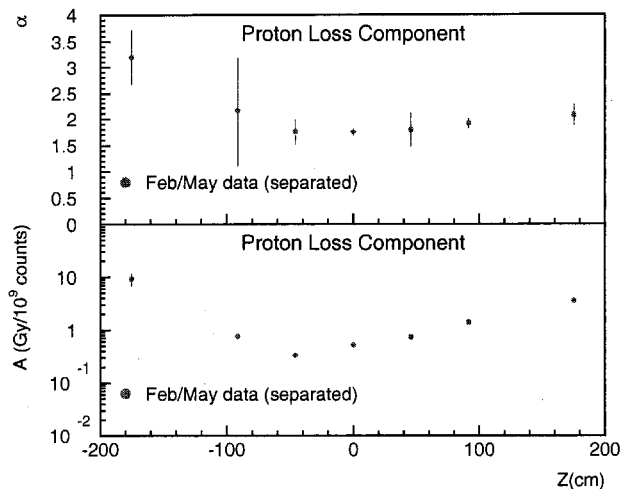


Fig. 6. Fit results for the proton loss component of the radiation field as a function of z separated from the first two exposure periods. The top figure shows the power law exponent, α ; the bottom figure shows the normalization, A .

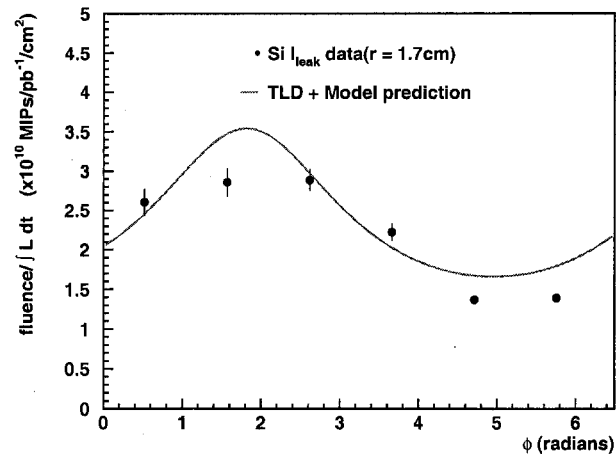


Fig. 7. Charged particle fluence rate as a function of ϕ for the innermost layers of silicon (L00). The points are calculations from leakage current data. The curve is a prediction based on TLD measurements.

show no position dependence in the central ($|z| < 100 \text{ cm}$) region of the tracking volume. We separate the ionizing radiation into a component from beam losses and another from collisions. The fraction of the radiation arising from the collision component is observed to increase with improved beam conditions. We model the ionizing radiation field using a simple power law in $1/r$, where r is the distance from the beam axis. Agreement within 10% is seen when comparing the particle fluxes obtained from the TLD measurements and leakage current measurement from the innermost silicon sensors.

REFERENCES

- [1] C. Leroy, S. Bates, B. Dezillie, M. Glaser, F. Lemeilleur and I. Trigger, Nucl. Instr. Meth. **A388**, (289) 1997; F. Lemeilleur, M. Glaser, E. H. Heijne, P. Jarron and E. Occelli, IEEE Trans. Nucl. Sci. **39**, (551) 1992;
- [2] D. Amidei, *et al.* Nucl. Instr. and Meth. **A350** (73) 1994.

- [3] Saint-Gobain Crystals, 6801 Cochran Rd, Solon, OH 44139, USA.
- [4] F. Krueger, S. Hawke, "Calibration and On-Axis Characterization of the Source Projector Facility at the Radiation Physics Calibration Facility", Fermilab Radiation Physics internal note 121, January 1996.
- [5] Oak Ridge Calibration Facility, Oak Ridge, TN.
- [6] National Nuclear Data Center, Brookhaven National Laboratory, Upton, NY 11973-5000 (<http://www.nndc.bnl.gov>).
- [7] Harshaw model 2000 TLD reader: Thermo RMP, 6801 Cochran Road, Solon, OH 44139, USA. The model 2000 TLD reader used for these measurements was modified to extend the reading cycle to 10 seconds.
- [8] J. Elias, *et al.* Nucl. Instr. and Meth. **A441** (366-373), 2000. D. Acosta, *et al.* Nucl. Instr. and Meth. **A461** (540-544), 2001.

ACKNOWLEDGMENT

The authors would like to thank the staff and technicians of the Fermilab and Oak Ridge Radiation Physics Calibration facility and the Fermilab Silicon Detector facility for their assistance. Finally we acknowledge support from the CDF operations department and the Fermilab beams division for many useful discussions and assistance.